Gravitational memory of Neutrinos

Darsh Kodwani,[1, 2, *] Ue-Li Pen,[1, 3, 4, 5, †] and I-Sheng Yang[1, 5, ‡]

[1]*Canadian Institute of Theoretical Astrophysics, 60 St George St, Toronto, ON M5S 3H8, Canada.*
[2]*University of Toronto, Department of Physics, 60 St George St, Toronto, ON M5S 3H8, Canada.*
[3]*Canadian Institute for Advanced Research, CIFAR program in Gravitation and Cosmology.*
[4]*Dunlap Institute for Astronomy & Astrophysics, University of Toronto,*
AB 120-50 St. George Street, Toronto, ON M5S 3H4, Canada.
[5]*Perimeter Institute of Theoretical Physics, 31 Caroline Street North, Waterloo, ON N2L 2Y5, Canada.*

We calculate the gravitational memory effect when a spherically symmetric shell of energy passes through a spacetime region. In particular, this effect includes a longitudinal component, such that two radially separated geodesics pick up a relative velocity proportional to their separation. Such a measurement will allow us to obtain the total energy released by a supernova explosion in the form of neutrinos. We study the possibility to measure such an effect by space-based interferometers such as LISA and BBO, and also by astrophysical interferometers such as pulsar scintillometry.

---

[*] dkodwani@physics.utoronto.ca
[†] pen@cita.utoronto.ca
[‡] isheng.yang@gmail.com

I.   INTRODUCTION AND SUMMARY

The recent detection of gravitational waves [1] has proved that gravitational waves leave an oscillating pattern in the amplitude of waveforms measured at detectors such as LIGO. It is also known that this is not the only effect that is potentially detectable. Strong gravitational waves imply a large flow of energy. Just like any other flow of energy, it leads to a gravitational memory effect [2, 3].

The memory effect discussed in [2, 3] causes permanent relative displacements between geodesics. It contains only transverse-traceless components and can leave an imprint in an interferometer. In this paper, we will introduce another memory effect that is different in two ways:

- It has a longitudinal component. The transverse-traceless limitation only applies to freely-propagating changes of the metric (i.e gravitational waves). While coupled to matter, which often have longitudinal (density) waves, it is natural to have an accompanying longitudinal change in the metric.

- Instead of displacements, it causes permanent changes in relative velocities between geodesics, with magnitudes proportional to their separations.

In terms of the dynamics, a change in velocity is higher order than a change in distance. This however does not mean that our effect is harder to measure. The conventional gravitational memory effect needs a physical event that significantly breaks spherical symmetry to be detectable whereas our effect does not and therefore it can occur more generally. In addition, a change in velocity implies a distance change that grows in time even after the initial effect. That is an advantage for some detection methods.

We will present a simple and natural occurrence of this effect. During a supernova explosion (SNe), most of the energy is released in a highly relativistic shell of neutrinos. As illustrated in Fig.1, when a neutrino shell passes through, the three free-falling points A, B and C, will pick up different velocities due to the change of geometry. If AB and BC are two arms of an interferometer, we will see a time-dependent change after the shell passes through. Note that this is purely a geometric change which happens even without the three actual objects. We will demonstrate this by showing that it is possibility to detect the same effect using pulsar interferometry, in which two parallel light rays get different time-delays after being hit by a neutrino shell.

The SKA telescope is expected to detect thousands of pulsars, [4], and one of them might be close enough to a SN explosion to provide us with a good estimation of the total energy in the neutrino shell of the explosion. Currently there is no other way to obtain such information. Thus in addition to direct neutrino detections such as in Super-Kamiokande [5], this memory effect can provide a new handle on constraining the explosion mechanism.

The rest of the paper is organized as follows. In section II we derive the change in velocities with the Israel Junction Conditions (IJC) [6], treating the neutrino shell as a co-dimension-one delta function. In section III we discuss potential observation of such an effect by experiments that are currently being planned such as LISA and BBO. The final section IV discusses how an astrophysical interferometer formed by pulsar scintillometry can measure the same effect.
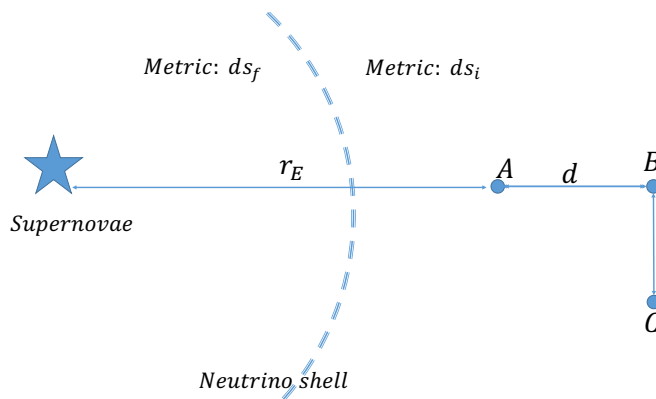

FIG. 1. Schematic of the effect being considered by a neutrino shell passing through the interferometer. The points A, B, C represent ends of the interferometer of arm length d. The three points A, B and C will pick up velocities v_A, v_B and v_C respectively after the shell crosses them. They are all different since they cross the shell at different locations.

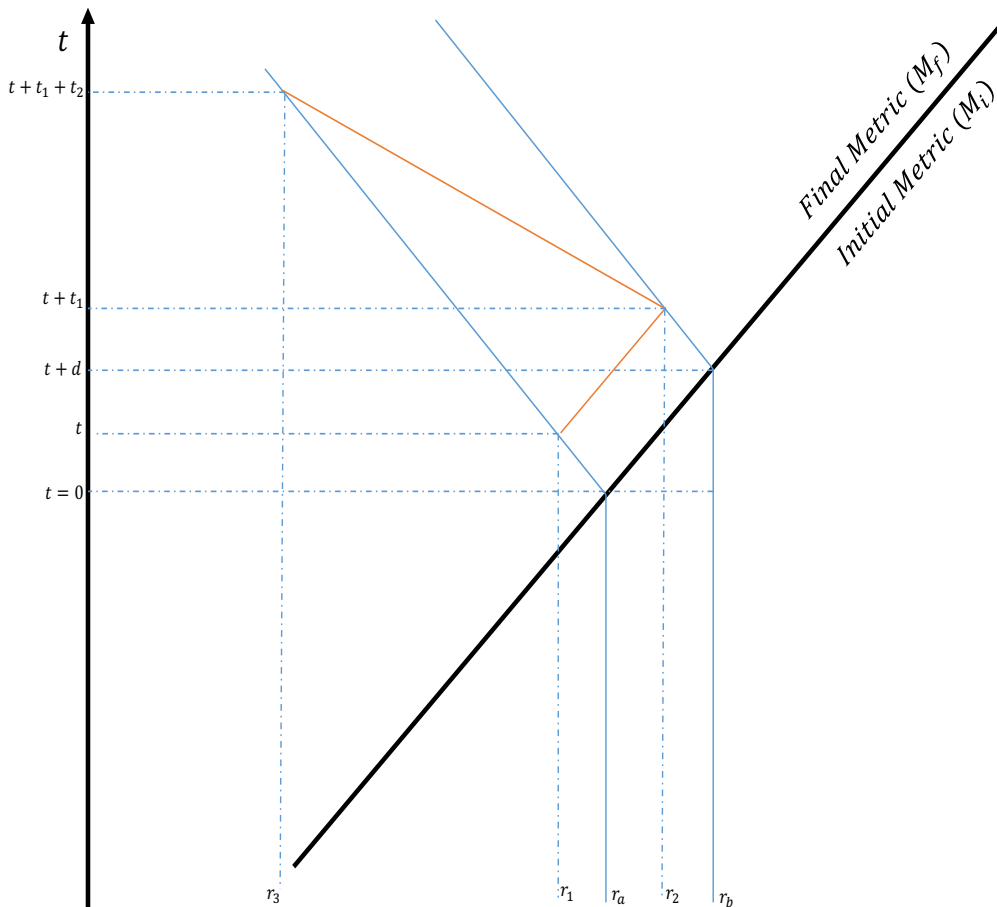## II. CHANGE IN RELATIVE VELOCITY

FIG. 2. Schematic of a spacetime diagram showing the paths of photons that are used in the interferometer to measure the change in the length of the interferometer arms. The orange lines represent the photon trajectories. The solid blue lines represent the trajectories of the two points A and B in figure 1. The dark black line is the null trajectory of the neutrino shell.

We assume the geometry of the spacetime is governed by the SN progenitor star. We assume the star is not rotating very rapidly and thus the surrounding spacetime is parametrized by the Schwarzschild metric,

$$ds_i^2 = -\left(1 - \frac{2M_i}{r}\right)dt_i^2 + \left(1 - \frac{2M_i}{r}\right)^{-1}dr^2 + r^2 d\Omega_2^2, \tag{1}$$

where are working in units with $G = c = 1$. After the star explodes, it emits a shell of neutrinos carrying energy δM. The metric surrounding the original star then changes since the mass has changed. In particular the i index used above to denote the "initial" metric is replaced by f to denote the "final" metric with a smaller mass $M_f = M_i - \delta M$. Notice that the time component of the metric is different in both geometries whereas the radial component is the same as it corresponds to the radius of a two sphere separating the two geometries. Since we are describing the shell as a delta function travelling at roughly the speed of light it will follow a null geodesic. The null vector of the shell can be written in both metrics as follows[1]

$$\Sigma^\mu_{(i,f)} = \left(\left(1 - \frac{2M_{(i,f)}}{r}\right)^{-1}, 1, 0, 0\right). \tag{2}$$

---

[1] One could write this vector in different ways and still have it satisfy the null normalization condition, however, the fact the shell has some surface area with a *fixed* radius, the two vectors must have the same radial component and this enforces the given form of the time component.

We choose a coordinate chart in which the interferometer points are initially at rest (denoted by the points A, B, C in figure 1) and are described by the following geodesic

$$\zeta_i^\mu = \left(\left(1 - \frac{2M_i}{r}\right)^{-\frac{1}{2}}, 0, 0, 0 \right). \tag{3}$$

The r will be different for points A, B and C as shown in figure 1. After the shell has crossed the points we expect ζ to have a velocity component. This can be found using the IJC,

$$g_{\mu\nu} \Sigma_{(i)}^\mu \zeta_{(i)}^\nu = \hat{g}_{\mu\nu} \Sigma_{(f)}^\mu \zeta_{(f)}^\nu, \tag{4}$$

where $\hat{g}_{\mu\nu}$ represents the metric of the "final" spacetime and $g_{\mu\nu}$ is the metric of the initial spacetime. This expression comes from demanding the continuity of geodesics from one geometry to another and was used in [7] to calculate a similar effect. Substituting Eqs (2, 3) into Eq (4) gives the final vector for the interferometer, to leading order,

$$\zeta_f^\mu = \left(\left(1 - \frac{2M_f}{r_{crossing}}\right)^{-\frac{1}{2}}, -\frac{\delta M}{r_{crossing}}, 0, 0 \right). \tag{5}$$

Note that $\frac{\delta M}{r_{crossing}}$ is a coordinate velocity and to convert to proper velocity it will need to be multiplied by a factor of $\left(1 - \frac{2M}{r_{crossing}}\right)^{\frac{1}{2}}$. $r_{crossing}$ is a fixed distance at which the shell crosses a point. For A it is r_E, for B it is $r_E + d$ and for C it is $\approx r_E + d$ as well.[2]

A. Distance change

1. The relationship between proper time and distance

The distance change is measured by an interferometer. The interferometer calculates the distance by sending photons to a target and measuring the time it takes for them to come back. To demonstrate this we consider the simple case shown in figure 3. Two freely falling points A and B are in the gravitational field of an object with mass M. The two points have a separation d between them at T_0. The distance of the first point from the mass M is R_0. The trajectories of the two points (as shown in figure (3)) are given by

$$R_A(t) = R_0 - \frac{1}{2} \frac{M}{R_0^2} t^2, \tag{6}$$

$$R_B(t) = R_0 - \frac{1}{2} \frac{M}{(R_0 + d)^2} t^2. \tag{7}$$

The time at which the photon reaches R_B is T. We can calculate T using the metric in Eq (1) with mass M. Setting $ds^2 = 0$ for the photons gives

$$\int_{T_0}^T dt = \int_{R_A}^{R_B} \left(1 - \frac{2M}{r}\right)^{-1} dr \tag{8}$$

We take $\frac{M}{r_0^2} \ll 1$ and so we can approximate that r doesn't change with time to do the integral,

$$T = R_B(T_0) - R_A(T_0) + 2M \ln\left(\frac{R_B(T_0) - 2M}{R_A(T_0) - 2M}\right). \tag{9}$$

---

[2] The exact expression is $r_E \left(1 + \frac{2d}{r_0} + \frac{2d^2}{r_0^2}\right)^{\frac{1}{2}}$ but we are working to leading order so we can make the given approximation.

Note that there is some ambiguity over what time the R's on the right hand side of Eq (9) should be evaluated at. Looking ahead to the problem we will construct in the later section, we assume[3] $T - T_0 \ll T_0$ and so to leading order we can evaluate the R's at T_0. If we only keep leading order terms in Eq (9), we can drop the log term as well.

$$T \approx d + \frac{1}{2}\frac{M}{(R_0 + d)^2}T_0^2 - \frac{1}{2}\frac{M}{R_0^2}T_0^2 = d + \mathcal{O}(R_0^{-3}). \tag{10}$$

The proper time $\tau = \left(1 - \frac{2M}{r}\right)^{\frac{1}{2}} T$. Thus we see that for a weak gravitational field, τ is the distance d to leading order. This shows that whenever we measure the proper time interval it takes for photons to travel a distance between two points, we are also measuring the distance between two points.
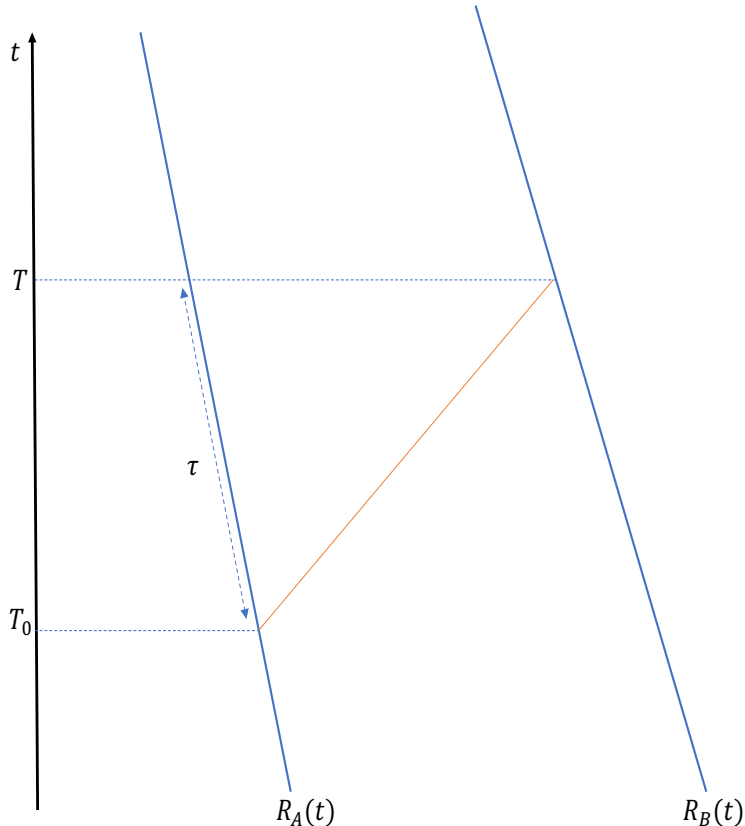

FIG. 3. Space-time diagram showing two points free falling towards a mass M. A photon is emitted from the point on the inside at time T_0 and is received at the outer point at time T. The dark blue lines parametrize the trajectories of the two points and the orange line represents the trajectory of the photon.

2. Full interferometric calculation

Now lets move on the more realistic case of the interferometer shown in figure 2. We parametrize the trajectory of each point in a piecewise form. For point A we have

----

[3] Note that $T - T_0 \sim \mathcal{O}(d)$.

$$r_A(t) = r_0 - \frac{1}{2}\frac{M}{r_0^2}t^2, \qquad\qquad (t \le 0)$$

$$= r_0 - \frac{1}{2}\frac{M-\delta M}{r_0^2}t^2 - \frac{\delta M t}{r_0}\left(1 - \frac{2(M-\delta M)}{r_0}\right)^{\frac{1}{2}}. \qquad (t > 0) \qquad (11)$$

$t = 0$ is defined to be the time when the shell crosses point A and the distance $r_A(0) = r_0$. For $t < 0$ the only term that contributes to the trajectory is the acceleration of point A towards mass M. For $t > 0$ there is still the acceleration term but the mass is different since the shell has carried δM away. Along with that there is a term that corresponds to the velocity change coming from the shell crossing. The trajectory of point B is given by.

$$r_B(t) = r_0 + d - \frac{1}{2}\frac{M}{(r_0+d)^2}t^2, \qquad\qquad (t \le d)$$

$$= r_0 + d - \frac{1}{2}\frac{M}{(r_0+d)^2}d^2 - \frac{1}{2}\frac{M-\delta M}{(r_0+d)^2}(t-d)^2 - \frac{1}{2}\frac{\delta M}{r_0+d}\left(1 - \frac{2(M-\delta M)}{r_0}\right)^{\frac{1}{2}}(t-d). \quad (t > d) \quad (12)$$

For $t < d$ there is just the acceleration of the point towards mass M. After $t > d$ the shell has crossed and now there is a change in distance in the time d (to leading order the shell takes time d to go from r_0 to $r_0 + d$) that the point is accelerating towards M. This is the second term in the expression. The other two terms correspond to the acceleration and velocity, respectively, of the point towards mass $M - \delta M$. Using these trajectories we can calculate how the distance between points A and B changes as a function of time.

A photon is released at time t after the shell has crossed point A. Using Eqs (11, 12) we can calculate the time, $\bar\tau$, it takes for this photon to go to point B and come back to point A. The full calculation is presented in the appendix. The leading order result is

$$\bar\tau = 2d - \frac{3(M-\delta M)d}{r_0} + \frac{2\delta M d}{r_0}. \qquad (13)$$

Note that there is no time dependence in this expression. In fact, the time dependence will come in at $\mathcal{O}(r_0^{-3})$ in this case.[4] As shown in section II A 1 this expression for τ will the leading order distance between A and B. The change in distance after shell crossing is

$$\Delta L_{AB} \equiv \bar\tau - 2d = -\frac{3(M-\delta M)d}{r_0} + \frac{2\delta M d}{r_0}. \qquad (14)$$

Since this is a permanent change in the distance - it is nothing but a memory effect. Next we show an effect which is much more interesting since it grows with time.

The interferometer arm that goes from B to C will see the distance between these two points change. In fact, this distance is much simpler to calculate. The points B and C will feel the same acceleration to M to leading order and so we can simply look at the change in velocities due to shell crossing. The velocities for points B, v_B, and C, v_C, have the same magnitudes to leading order but are pointing in slightly different directions. From the geometry of figure 1 we see that the relative change in velocity between the two points along the vertical direction will be $v_C \sin\theta$ where $\sin\theta \approx d/r_0$. The distance change between the two points, ΔL_{BC}, is therefore given by

$$\Delta L_{BC} = -\left(\frac{\delta M}{r_0+d}\left(1 - \frac{2M}{r_0+d}\right)^{\frac{1}{2}}\sin\theta\right)t$$

$$= -d\frac{\delta M}{r_0^2}t + \mathcal{O}(r_0^{-3}). \qquad (15)$$

Since they both fall toward the SN, they are getting closer to each other thus ΔL_{BC} is *decreasing*. Thus we have found a memory effect that increases with time. This effect is suppressed compared to ΔL_{AB} by a factor of r_0^{-1} but since it grows with time there will be times for which this effect will be dominant.

---

[4] See appendix where we show that there is no time dependence at second order.

III.   OBSERVATION WITH SPACE-BASED INTERFEROMETERS

Taking the generic form of the change in distance as $\Delta L \sim \frac{\delta M d}{r_E^2} t$ we can estimate the distance a SN would have to be from the interferometer to have an observable change in strain, which is a unitless number quantifying the amount of space-time distortion.

$$h \sim \frac{\Delta L}{d} \sim \frac{\delta M t}{r_E^2} \ . \tag{16}$$

Since our strain grows linearly with time, we do not expect detections from ground based experiments as for those setups the three points A, B, C cannot remain in free fall for a long enough amount of time such that the signal builds up to an observable value.

If we plot our effect on the strain-frequency diagram [8] that is usually used to compare different interferometers, it will be a 45-degree line. Thus the first point at which the sensitivity curve of a device crosses with a 45-degree line will give the best chance for our effect being detected. In all these estimations, we take δM to be a faction of a solar mass, and take the corresponding Schwarzschild radius to be $1 \ km$ for simplicity.

For LISA, the best observing frequency is $\sim 0.5 \times 10^{-2} Hz$ with a sensitivity in strain $\sim 10^{-21}$. Using Eq. (16), we can solve for the distance to the SN, r_E, for our effect to be detectable.

$$r_E = \left(\frac{\delta M}{h} t \right)^{\frac{1}{2}} \tag{17}$$

$$= \left(\frac{1 \ km}{10^{-21}} \times 10^7 \ km \right)^{\frac{1}{2}} \approx 10^{14} \ km = 10 \ ly. \tag{18}$$

This is clearly too close. It has been estimated that only once in 10^8 years will a SN go off within a distance of $30 \ ly$ [9].[5] By a naive volume scaling, an explosion within $10 \ ly$ only occurs once every billion years.

If we look at the Big Bang Observer (BBO) instead, the best observing frequency is $\sim 0.5 Hz$ with a sensitivity in strain $\sim 10^{-24}$. First of all, this frequency range does not have as many background signals from compact binaries, making it a much better device to measure our effect. The improved sensitivity gives a value for r_E of $\sim 100 \ ly$. This is a factor of 10^3 increase in the volume for detectable events, thus improves the expectation of one SN that is within $10 \ ly$ to occur in less than a million years . That is unfortunately still a long shot.

In this type of simple estimation, we cannot go lower in the frequency. The exact duration of the neutrino-shell passage is not known, but we do no expect it to be much less than a second. Thus for higher frequencies, the co-dimension-one delta function approximation breaks down, and the effect will be weaker than Eq. (16).

Finally, we expect 2 to 3 SN per century in our galaxy and we can assume that the next SN would be at a distance comparable to the galactic diameter of $\sim 10^5 \ ly$. If we are going to measure such effect at $1 \ Hz$, Again using Eq. (16), we find

$$h = \frac{1 \ km \times \ (3 \times 10^8 \ m)}{(10^5 \ ly)^2} \sim 10^{-30} \ . \tag{19}$$

This requires a measurement of the strain that is six orders of magnitude better than BBO and is not yet achievable by interferometers that are currently being planned.

IV.   OBSERVATION WITH PULSAR SCINTILLATION

We learned from the previous section how difficult it is to measure the spacetime distortion. It is strongly suppressed by a factor of r_E^{-2}, which is proportional to the energy density of the shell when it reaches us. If we can have an interferometer much closer to the SN, the signal will be larger.

In this final section we discuss a possibility to do just that. It is known that the images of many astronomical bodies scintillate [10]. A general reason for scintillation is that due to scattering or lensing, we receive multiple light rays from the same objects. These light rays are very close to each other, so they cannot be individually resolved and have to interfere. The scintillation pattern we see is the time dependence of their interference. If we consider two

---

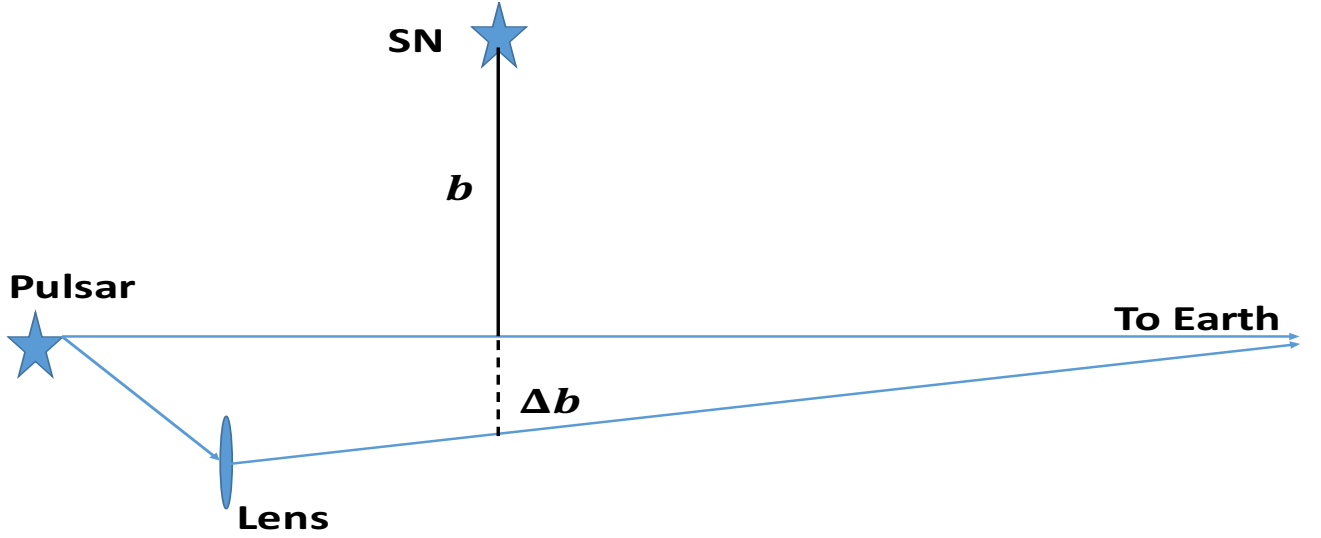[5] And if that happens, it might kill us.

FIG. 4. Geometry of the astrophysical interferometer formed by pulsar scintillometry. Due to scattering or lensing, the image we see is an interference pattern of two light rays represented by the blue lines. If the separation of the two light rays has a component along the longitudinal (radial) direction from the SN, the spacetime distortion of the neutrino shell will change the interference pattern we see. We draw the lens to be behind the SN, but it could have been in front of it and the effect is the same.

light rays from a faraway pulsar which happen to pass by a SN progenitor, as illustrated in Fig.4, they can probe the spacetime distortion when it explodes.

The scintillation/interference pattern is directly related to the path lengths of these light rays. The change in such path length during a SN explosion has been worked out in [11]

$$\Delta t = 2\delta M \left[\ln \left(1 + \frac{t^2}{b^2} \right) - \frac{t^2}{b^2 + t^2} \right]. \tag{20}$$

Here b is the impact parameter as shown in Fig.4, the shortest distance between the light ray and the SN. t is the proper time on earth, with $t = 0$ the time we directly observe the SN explosion. δM is the total energy of the neutrino shell, and Δt is the resulting time shift. A photon which should have reached the earth at time t, will arrive earlier at $(t - \Delta t)$ instead.

When the separation between two light rays has a component in the radial direction from the SN, Δb, there will be a nonzero relative change between their path lengths.

$$(\Delta t|_b - \Delta t|_{b+\Delta b}) \approx \frac{\partial \Delta t}{\partial b} \Delta b = -\frac{4\delta M t^4}{b(b^2 + t^2)^2} \Delta b \ . \tag{21}$$

We can see that this effect grows from zero and approaches an asymptotic value,

$$(\Delta t|_b - \Delta t|_{b+\Delta b}) \longrightarrow \frac{4\delta M \Delta b}{b} \ , \tag{22}$$

at a characteristic time scale given by b.

We estimate b by assuming that the next SN is somewhere near the galactic centre. A sample of ~ 9000 pulsars from the SKA catalog in [4] shows that among those pulsars, the shortest b is about $10\ ly \sim 10^{14}\ km$. Δb is related to the scattering-broadening of images. We use the data from [12] that was observed on a scattering screen near the galactic

centre. Scaling the frequency to 1 GHz which is usually a good window to observe pulsar signals. We found that such a scattering screen can produce images separated by $\Delta b \sim 1000 A.U. \sim 10^{10}\ km$. We again use $\delta M \sim 1\ km$, and combining all these numbers we get $(\delta M \Delta b/b) \sim 1\ m$. This is comparable to the wavelength at 1 GHz, thus making the change in interference pattern easy to detect. Therefore, if we can monitor the pulsar scintillation pattern over ten years after a SN explosion we should see an order one change in the scintillation pattern predicted by Eq. (21).

ACKNOWLEDGMENTS

Appendix A: Proper time for a photon going from point A to B and coming back

In this calculation we first calculate the time, t_1, it takes for the photon released at time t from point A to reach point B. Then we calculate the time, t_2, it takes for the photon to come back to point A. The quantities are clearly defined in figure 2. The final result is obtained by adding these times and converting to proper time.

$$
\begin{aligned}
t_1 &= d + \frac{1}{2}\frac{M-\delta M}{r_0^2}t^2 + \frac{\delta M}{r_0}\left(1 - \frac{2(M-\delta M)}{r_0}\right)^{\frac{1}{2}}t - \frac{1}{2}\frac{M}{(r_0+d)^2}d^2 - \frac{1}{2}\frac{M-\delta M}{(r_0+d)^2}(t+t_1-d)^2 - \frac{\delta M}{r_0+d}(t+t_1-d) \\
&\quad - \frac{Md}{r_0^2}(t+t_1-d) \\
&= d - \frac{1}{2}\frac{Md^2}{r_0^2} - \frac{M-\delta M}{r_0^2}dt + \mathcal{O}(r_0^{-3})
\end{aligned}
\tag{A1}
$$

where we used $t_1 = d + \mathcal{O}(r_0^{-1})$. Similarly we calculate the time, t_2, it takes for a photon to go from r_B to r_A.

$$
\begin{aligned}
t_2 &= d + \frac{1}{2}\frac{M-\delta M}{r_0^2}(t+t_1+t_2)^2 + \frac{\delta M}{r_0}\left(1 - \frac{2(M-\delta M)}{r_0}\right)^{\frac{1}{2}}(t+t_1+t_2) - \frac{1}{2}\frac{M-\delta M}{(r_0+d)^2}(t+t_1-d)^2 \\
&\quad - \frac{\delta M}{r_0+d}\left(1 - \frac{2(M-\delta M)}{r_0+d}\right)^{\frac{1}{2}}(t+t_1-d) - \frac{Md}{(r_0+d)^2}(t+t_1-d) \\
&= d + \frac{2\delta Md}{r_0} + \frac{2\delta M^2 d}{r_0^2} + 2\frac{M-\delta M}{r_0^2}d^2 - 2\frac{\delta M(M-\delta M)d}{r_0^2} + \frac{M-\delta M}{r_0^2}dt + \mathcal{O}(r_0^{-3})
\end{aligned}
\tag{A2}
$$

Lets convert these coordinate times into proper times,

$$
\begin{aligned}
t_1' &= \left(1 - \frac{2(M-\delta M)}{r_0}\right)t_1 \\
&= d - \frac{M-\delta M}{r_0}d - \frac{1}{2}\frac{Md^2}{r_0^2} - \frac{M-\delta M}{r_0^2}dt + \mathcal{O}(r_0^{-3})
\end{aligned}
\tag{A3}
$$

and for t_2' we get

$$
\begin{aligned}
t_2' &= \left(1 - \frac{2(M-\delta M)}{r_0+d}\right)t_2 \\
&= d + \frac{2\delta Md}{r_0} + \frac{2\delta M^2 d}{r_0^2} + \frac{2(M-\delta M)d^2}{r_0^2} + \frac{M-\delta M}{r_0^2}dt - \frac{2(M-\delta M)d}{r_0} - \frac{6\delta M(M-\delta M)d}{r_0^2} + \frac{2(M-\delta M)d^2}{r_0^2} + \mathcal{O}(r_0^{-3})
\end{aligned}
\tag{A4}
$$

giving the total travel time

$$\bar{\tau} \equiv t_1' + t_2' = 2d - \frac{3(M - \delta M)d}{r_0} + \frac{2\delta M d}{r_0} - \frac{1}{2}\frac{Md^2}{r_0^2} + \frac{2\delta M^2 d}{r_0^2} + \frac{4(M - \delta M)d^2}{r_0^2} - \frac{6\delta M(M - \delta M)d}{r_0^2} + \mathcal{O}(r_0^{-3}) \quad \text{(A5)}$$

so we see there is no time dependence.

[1] B. P. Abbott *et al.* (LIGO Scientific Collaboration and Virgo Collaboration), Phys. Rev. Lett. **116**, 061102 (2016).
[2] D. Christodoulou, Phys. Rev. Lett. **67**, 1486 (1991).
[3] K. S. Thorne, Phys. Rev. D **45**, 520 (1992).
[4] D. R. Lorimer, *Neutron Stars and Pulsars: Challenges and Opportunities after 80 years*, IAU Symposium, **291**, 237 (2013), arXiv:1210.2746.
[5] M. Malek *et al.* (Super-Kamiokande Collaboration), Phys. Rev. Lett. **90**, 061101 (2003).
[6] W. Israel, Nuovo Cim. **B44S10**, 1 (1966).
[7] D. Kodwani, U.-L. Pen, and I.-S. Yang, Phys. Rev. D **93**, 103006 (2016).
[8] C. J. Moore, R. H. Cole, and C. P. L. Berry, Class. Quant. Grav. **32**, 015014 (2015), arXiv:1408.0740 [gr-qc].
[9] J. R. Ellis and D. N. Schramm, (1993), arXiv:hep-ph/9303206 [hep-ph].
[10] R. Narayan, Philosophical Transactions: Physical Sciences and Engineering **341**, 151 (1992).
[11] K. D. Olum, E. Pierce, and X. Siemens, Phys. Rev. **D88**, 043005 (2013), arXiv:1305.3881 [gr-qc].
[12] G. C. Bower, A. Deller, P. Demorest, A. Brunthaler, R. Eatough, H. Falcke, M. Kramer, K. J. Lee, and L. Spitler, Astrophys. J. **780**, L2 (2014), arXiv:1309.4672 [astro-ph.GA].